Generalized Representation of Phase Derivatives for Regular Signals

Cédric Cornu, Srdjan Stanković, Cornel Ioana, André Quinquis, LJubiša Stanković

Abstract— **This paper introduces a new generalized complex lag moment which produces joint time-"phase derivatives" distributions. For the choice of the time-"first order phase derivative" which stands for time-frequency representation, this distribution can be seen as a form of the Wigner-Ville distribution. Moreover, this generalization leads to distributions with highly reduced inner interferences caused by the nonlinearity of the signal's phase. It can also be seen as a polynomial distribution since the N^{th} order distribution produces no inner interferences for polynomial phase law of order N. Implementation of these distributions is addressed. The results are illustrated by examples.**

I. Introduction

A General form of complex lag distributions, that estimates any order of instantaneous phase derivative, is introduced. This class of distributions is based on complex lag arguments. It will be referred to as a general form of the complex time distributions. Beside the fact that these distributions provide estimation of an arbitrary order of instantaneous phase derivative, high concentration of the distributions can be achieved. Since the first phase derivative is the instantaneous frequency, time-frequency distributions follow as a special case of this class of distributions, [1], [2]. Time-frequency distributions, introduced by the proposed approach, are highly concentrated in the time-frequency plane providing an accurate instantaneous frequency estimation, even in the case of significant instantaneous frequency variation within only a few signal samples. Recently, O'Shea analyzed the second order phase derivative, i.e. the Instantaneous Frequency Rate (IFR), [3]. The estimation introduced in [3] can be obtained with a slight modification of a particular form of the generalized complex lag distribution. In addition, better instantaneous frequency rate concentration can be achieved by using higher order time frequency rate distributions belonging to the proposed class of distributions. Distributions providing the third instantaneous phase derivative are also introduced and analyzed.

The paper is organized through five sections. The concept and theory of the proposed class of distributions are presented in Section II. The theory is illustrated by various examples in Section III. The problem of numerical implementation is considered in Section IV. The most interesting specific distributions, belonging to the proposed class of distributions, are illustrated in Section V. Special attention is devoted to the cases of the first, the second and the third phase derivatives. In the case of first phase derivative (instantaneous frequency), the superiority of the proposed approach is illustrated by introducing the sixth order distribution that estimates the instantaneous frequency, even when it could not be achieved by other time-frequency tools.

II. Instantaneous phase derivatives

A. Concept

The ideal representation of an arbitrary Instantaneous Phase Derivative (IPD), for signals of the form $Ae^{j\Phi(t)}$, can be written in the form:

$$IPD_K(t,\Omega) = \delta(\Omega - \Phi^{(K)}(t)), \qquad (1)$$

where Ω is the axis which corresponds to the K^{th} derivative of the phase function $\Phi(t)$. The distribution which provides this representation will be called, in general, the ideal time-"phase derivatives" distribution. Note that, for $K =$

IEEE Transactions on Signal Processing, Vol. 55, No. 10, Oct. 2007.

1, the instantaneous frequency representation is obtained as:

$$IPD_1(t,\omega) = \delta(\omega - \Phi'(t)), \tag{2}$$

where $\Omega \equiv \omega$ and $\Phi'(t)$ stands for the first phase derivative, i.e. instantaneous frequency. The well known time-frequency distributions, [1], [2], could be used for this representation.

For $K = 2$ instantaneous frequency rate follows:

$$IPD_2(t,\Omega) = \delta(\Omega - \Phi^{(2)}(t)), \tag{3}$$

where Ω is the frequency rate axis. Instantaneous frequency rate estimation can be provided by using, recently defined, time-"frequency rate" representation, [3].

Note that these two special cases have already been studied (especially the case $K = 1$) while the case $K = 3$ has not been considered yet. A reason for this could be the elaborate forms of distributions even for the first two cases. Namely, ideal representations given by equations (2) and (3) can not, generally, be achieved by using any time-frequency or time-"frequency rate" distribution. Terms which cause the distribution spread, around the instantaneous phase derivative, are inner interference terms. For $K = 1$, they depend on $\left\{\Phi^{(i)}(t)\right\}_i$, for $i \geq 2$. Note that, for the spectrogram we have $i = 2, 3, ...,$ while for the Wigner distribution we have $i = 3, 5, 7, ...,$ [4].

Distribution proposed in the next section provides not only an arbitrary instantaneous phase derivative representation, but also high distribution concentration.

Observe that energetic distributions should provide representation in the form:

$$IPD_K(t,\Omega) = A^2\delta(\Omega - \Phi^{(K)}(t)), \tag{4}$$

where A is the amplitude of the signal $s(t) = Ae^{j\Phi(t)}$. Thus, the signal energy is concentrated along the K^{th} phase derivative.

A general form of the distribution which provides instantaneous K^{th} phase derivative is introduced in the next subsection.

B. Introducing generalized complex lag time-"phase derivatives" distribution

In the sequel we will show that, by using the complex-lag argument concept, a set of new distributions can be defined. In order to reduce inner interferences in time-frequency representation of highly nonstationary signals, the complex lag argument was introduced in [4]. In this section, we prove that the distributions based on Generalized Complex lag Moment (GCM) provide the representation of arbitrary instantaneous phase derivatives. The distributions as the short time Fourier transform, the Wigner-Ville distribution (WVD), or O'Shea's time-frequency rate estimator, can be obtained as special cases. However, it is important to emphasize that this concept provides new, highly concentrated, distributions along the arbitrary phase derivative.

Let us consider a signal in the form:

$$s(t) = Ae^{j\Phi(t)}. \tag{5}$$

In order to obtain distribution concentrated along K^{th} phase derivative, we define a complex moment[1] as:

$$\underline{GCM}_N^K[s](t,\tau) = \prod_{k=0}^{N-1} s^{\omega_{N,k}^{N-K}}\left(t + \omega_{N,k}\tau\right), \tag{6}$$

where $\omega_{N,k} = e^{j2\pi k/N}$. The phase function of $\underline{GCM}_N^K$ is:

$$Angle\left[\underline{GCM}_N^K[s](t,\tau)\right] = \\ = \sum_{k=0}^{N-1} \Phi\left(t + \omega_{N,k}\tau\right)\omega_{N,k}^{N-K}. \tag{7}$$

By expanding Φ into Taylor's series, the above equation can be written as:

$$Angle\left[\underline{GCM}_N^K[s](t,\tau)\right] = \\ = \sum_{k=0}^{N-1}\sum_{i=0}^{+\infty} \Phi^{(i)}(t)\frac{\omega_{N,k}^i}{i!}\tau^i\omega_{N,k}^{N-K}. \tag{8}$$

Having in mind that:

$$\sum_{k=0}^{N-1}\omega_{N,k}^p = \begin{cases} N & \text{if } p = 0 \pmod N \\ 0 & \text{if not} \end{cases}$$

[1]Complex variable analysis provide the following derivative formula: $\Phi^{(k)}(t) = \frac{k!}{2\pi\tau^k}\int_0^{2\pi}\Phi(t + \tau e^{j\theta})e^{-jk\theta}d\theta$. The equation (6) is introduced in order to produce the phase in discrete domain, (7), that is analog with the previous formulation.

only the terms for $i=K, K+N, K+2N, ..., K+kN, ...$ will remain in (8). Therefore, we have:

$$\sum_{k=0}^{N-1} \Phi(t+\omega_{\mathrm{N,k}}\tau)\omega_{\mathrm{N,k}}^{\mathrm{N-K}} =$$

$$= N\sum_{k=0}^{+\infty} \Phi^{(\mathrm{Nk+K})}(t)\frac{\tau^{\mathrm{Nk+K}}}{(Nk+K)!}, \qquad (9)$$

which can be written as:

$$\sum_{k=0}^{N-1} \Phi(t+\omega_{N,k}\tau)\omega_{N,k}^{N-K} =$$

$$= \Phi^{(K)}(t)\frac{N\tau^K}{K!} + \underline{Q}(t,\tau), \qquad (10)$$

where the remainder $\underline{Q}(t,\tau)$ is:

$$\underline{Q}(t,\tau) = N\sum_{k=1}^{\infty} \Phi^{(Nk+K)}(t)\frac{\tau^{Nk+K}}{(Nk+K)!}. \quad (11)$$

If we want to obtain a distribution concentrated along $\Phi^{(K)}(t)$, we have to linearize the first term in (10) with respect to variable τ. Thus, the GCM should be of the form:

$$GCM_N^K[s](t,\tau) =$$

$$= \prod_{k=0}^{N-1} s^{\omega_{N,k}^{N-K}}\left(t+\omega_{N,k}\sqrt[K]{\frac{K!}{N}}\tau\right). \qquad (12)$$

After this lag warping, the phase function of the moment becomes:

$$Angle\left[GCM_N^K[s](t,\tau)\right] = \Phi^{(K)}(t)\tau + Q(t,\tau), \qquad (13)$$

where:

$$Q(t,\tau) =$$

$$= N\sum_{k=1}^{+\infty} \Phi^{(Nk+K)}(t)\frac{\tau^{\frac{Nk}{K}+1}}{(Nk+K)!}\left(\frac{K!}{N}\right)^{\frac{Nk}{K}+1}. \qquad (14)$$

The Fourier transform of the generalized complex moment produces the generalized complex lag distribution:

$$GCD_N^K[s](t,\omega) = \mathfrak{F}_\tau\left[GCM_N^K[s](t,\tau)\right]$$

$$= \mathfrak{F}_\tau\left[e^{j\Phi^{(K)}(t)\tau}e^{jQ(t,\tau)}\right]$$

$$= \delta(\omega-\Phi^{(K)}(t)) \underset{\omega}{*} \mathfrak{F}_\tau\left[e^{jQ(t,\tau)}\right], \qquad (15)$$

where $Q(t,\tau)$ is the spread factor of the distribution. In the ideal case, it should be zero. We observe that the first term appearing in this factor is the phase derivative of order $K+N$, the second one is of order $K+2N$, etc. Thus, the parameter N highly affects the factor $Q(t,\tau)$. It can be concluded that a high value of N reduces interferences, since $Q(t,\tau)$ is reduced. In order to give a more comprehensive overview of this theoretical framework, several specific distributions and illustrative examples are given in the next section.

III. Some specific distributions belonging to the generalized complex lag distribution

A. Case $K=1$: instantaneous frequency representation - time-frequency distributions

Taking $K=1$, we focus on the instantaneous frequency. Observing that $\omega_{N,k}^{N-1} = \omega_{N,k}^*$, moment (12) becomes :

$$GCM_N^1[s](t,\tau) = \prod_{k=0}^{N-1} s^{\omega_{N,k}^*}\left(t+\frac{\omega_{N,k}}{N}\tau\right). \qquad (16)$$

Depending on the parameter N, various forms of time-frequency distribution moments can be obtained. Let us begin with the first one, i.e. $N=1$:

$$GCM_1^1[s](t,\tau) = s(t+\tau)$$

$$Q(t,\tau) = \Phi^{(2)}(t)\frac{\tau^2}{2!} + \Phi^{(3)}(t)\frac{\tau^3}{3!} + \dots$$

Here, the associated distribution is the short time Fourier transform (if a lag window is assumed). In the spread factor $Q(t,\tau)$, all phase derivatives of order 2 and higher are implied. Thus, the short-time Fourier transform is well suited only for sinusoids localization.

For $N=2$ we have:

$$GCM_2^1[s](t,\tau) = s(t+\frac{\tau}{2})s^{-1}(t-\frac{\tau}{2})$$

$$Q(t,\tau) = \Phi^{(3)}(t)\frac{\tau^3}{3!\,2^2} + \Phi^{(5)}(t)\frac{\tau^5}{5!\,2^4} + \dots$$

This leads to a Wigner-Ville like distribution, with a difference in the second exponent of the moment which is -1 instead of a conjugate. However, both have the same effect on the phase. The first term appearing in $Q(t,\tau)$ is related to the third derivative. Indeed, the Wigner-Ville distribution is well suited for time frequency representation of linear frequency modulations.

Suppose now $N = 4$:

$$GCM_4^1[s](t,\tau) =$$

$$= s(t+\frac{\tau}{4})s^{-1}(t-\frac{\tau}{4})s^{j}(t-j\frac{\tau}{4})s^{-j}(t+j\frac{\tau}{4})$$

$$Q(t,\tau) = \Phi^{(5)}(t)\frac{\tau^5}{5!\,4^4} + \Phi^{(9)}(t)\frac{\tau^9}{9!\,4^8} + \dots$$

We observe that the same complex lag moment as the one introduced in [4] is obtained. The complex time distribution (CTD) is ideally concentrated for polynomial instantaneous frequency laws of order 3 or less. However, it has been shown that it is still highly efficient for polynomial phase of order greater than 4, since the derivative coefficients in the spread factor decay rapidly. For even N values, -1 is always a root of the unity and the exponent with value -1 can be replaced with a conjugate, since the effect on the phase function will be the same.

Hereafter, $\widetilde{GCM_N^K}$ will denote the moment GCM_N^K modified by replacing exponents -1 with conjugates. Thus, according to this notation the complex time distribution defined in [4] is $\widetilde{GCD_4^1}$. We can see that: $\int GCD_N^1[s]d\omega = 1$ and $\int \widetilde{GCD_N^1}[s]d\omega = |s(t)|^2$. Of course, it is possible to choose a higher value for N. For $N = 6$, highly concentrated, the sixth order time-frequency distribution moment is obtained:

$$\{\omega_{6,k}\}_{k=0..5} = \left\{1; e^{j\frac{\pi}{3}}; e^{j\frac{2\pi}{3}}; -1; e^{j\frac{-2\pi}{3}}; e^{j\frac{-\pi}{3}}\right\}$$

$$GCM_6^1[s](t,\tau) = \prod_{k=0}^{5} s^{\omega_{6,k}^*}\left(t+\frac{\omega_{6,k}}{6}\tau\right)$$

$$Q(t,\tau) = \Phi^{(7)}(t)\frac{\tau^7}{7!\,6^5} + \Phi^{(13)}(t)\frac{\tau^{13}}{13!\,6^{12}} + \dots$$

The first derivative appearing in the factor $Q(t,\tau)$ is of order 7. It means that a polynomial phase of order 6 or less will not produce any interferences in this distribution. For other signals, the interferences will be highly reduced, as a consequence of the very fast decreasing coefficients.

B. Case $K = 2$: time-"frequency rate" representation

A general form of the time-frequency rate distribution moments, with complex lag argument is given by:

$$GCM_N^2[s](t,\tau) = \prod_{k=0}^{N-1} s^{\omega_{N,k}^{N-2}}\left(t+\omega_{N,k}\sqrt[2]{\frac{2}{N}\tau}\right). \quad (17)$$

For $N = 2$ in (17), follows:

$$GCM_2^2[s](t,\tau) = s\left(t+\sqrt{\tau}\right)s\left(t-\sqrt{\tau}\right). \quad (18)$$

Relation (18) should be compared to the IFR representation and estimator introduced by O'Shea ([3]):

$$CPD(t,\Omega) = \int_0^{+\infty} s(t+\tau)s(t-\tau)e^{j\Omega\tau^2}d\tau, \quad (19)$$

$$IFR(t) = \underset{\Omega}{argmax}\left[CPD(t,\Omega)\right]. \quad (20)$$

By using the time warping operation $\tau \to \sqrt{\tau}$, and the Fourier transform instead of the polynomial Fourier transform, the distribution GCD_2^2 is obtained.

Taking $N = 4$, we will introduce a new, fourth order, time-"frequency rate" distribution moment:

$$GCM_4^2[s](t,\tau) = s\left(t+\sqrt{\frac{\tau}{2}}\right)s\left(t-\sqrt{\frac{\tau}{2}}\right)$$

$$\times s^{-1}\left(t+j\sqrt{\frac{\tau}{2}}\right)s^{-1}\left(t-j\sqrt{\frac{\tau}{2}}\right), \quad (21)$$

or:

$$\widetilde{GCM_4^2}[s](t,\tau) = s\left(t+\sqrt{\frac{\tau}{2}}\right)s\left(t-\sqrt{\frac{\tau}{2}}\right)$$

$$\times s^*\left(t+j\sqrt{\frac{\tau}{2}}\right)s^*\left(t-j\sqrt{\frac{\tau}{2}}\right). \quad (22)$$

The sixth order time-"frequency rate" distribution moment is obtained by taking $N=6$:

$$GCM_6^2[s](t,\tau)=\prod_{k=0}^{5}s^{\omega_{6,k}^4}\left(t+\omega_{6,k}\sqrt[2]{\frac{\tau}{3}}\right). \quad (23)$$

C. Case $K=3$: instantaneous third phase derivative representation

Note that, if we want to obtain distributions concentrated around third phase derivative, the parameter N must be $N\geq K$. Taking $N=3$, we have:

$$\{\omega_{3,i}\}=\left\{1,e^{j2\pi/3},e^{-j2\pi/3}\right\},$$

$$GCM_3^3[s](t,\tau)=\prod_{k=0}^{2}s\left(t+\omega_{3,k}\sqrt[3]{2\tau}\right). \quad (24)$$

It is easy to conclude that for $N=4$, better distribution concentration can be achieved. In this case we obtain the fourth order distribution moment:

$$GCM_4^3[s](t,\tau)=\prod_{k=0}^{3}s^{\omega_{4,k}}\left(t+\omega_{4,k}\sqrt[3]{\frac{3\tau}{2}}\right). \quad (25)$$

Taking $N=6$, the sixth order distribution moment is introduced:

$$GCM_6^3[s](t,\tau)=\prod_{k=0}^{5}s^{(-1)^k}\left(t+\omega_{6,k}\sqrt[3]{\tau}\right). \quad (26)$$

IV. GCD Implementation

A. Analytical continuation

Computation of the signal's value in the complex plane must be done, based on the real signal samples. In mathematics, this concept is known as analytical continuation, [5]. A function $s(t)$ is said to be analytical if it can be written as a power series within a convergence disk of radius $R\neq 0$, as:

$$s(t+j\tau)=\sum_{k=0}^{+\infty}\frac{s^{(k)}(t)}{k!}(j\tau)^k. \quad (27)$$

According to the Paley-Wiener theorem, a band limited signal can be regarded as an analytical function restricted on the real axis. Therefore, the analytical continuation of a band limited signal can be written using the inverse Fourier transform:

$$s(t+jm)=\int_{-\frac{B}{2}}^{+\frac{B}{2}}S(f)e^{-2\pi mf}e^{j2\pi ft}df. \quad (28)$$

With the previous formulation, and due to the finite support spectrum, it appears that the continuation could be computed for any band limited signal. However, in analysis we use windowed signals.

If $S(f)$ is the Fourier transform of a windowed signal by using the rectangular window, Fig.1.b, then it will have decay proportional to $1/f$. Therefore, due to the fast increasing exponential $e^{-2\pi mf}$, the analytical continuation, calculated via (28), could diverge. Problem is the same when the spectrum is obtained through the Discrete Fourier Transform (DFT):

$$s(n+jm)=\sum_{k=-\frac{N}{2}+1}^{\frac{N}{2}}S(k)e^{-2\pi mk}e^{j2\pi kn}. \quad (29)$$

The sampled spectrum involves repetition of the original signal in time. Necessary condition to have a fast decreasing spectrum is the continuity of all signal's derivatives, including repetition bounds. It can be achieved by applying a time axis warping to the signal. Let's suppose we have, $s\in C^\infty[-1,1]$ and $s(-1)\neq s(1)$. Let us also consider a warping function defined below:

$$w: t\rightarrow t_w=sin(\frac{\pi}{2}t). \quad (30)$$

The new defined function $\widetilde{s}(t)=s(w(t))$ is now periodical and C^∞ over the whole real axis, Fig.1.c. Moreover, one can expect its spectrum to be rapidly decreasing. To compute $s(t+jm)$, one must compute $\widetilde{s}(\tilde{t}+j\tilde{m})$, which is $\widetilde{s}(\frac{2}{\pi}asin(t+jm))$, from the spectrum of $\widetilde{s}$. The correspondence between the complex planes is illustrated in Fig. 2.

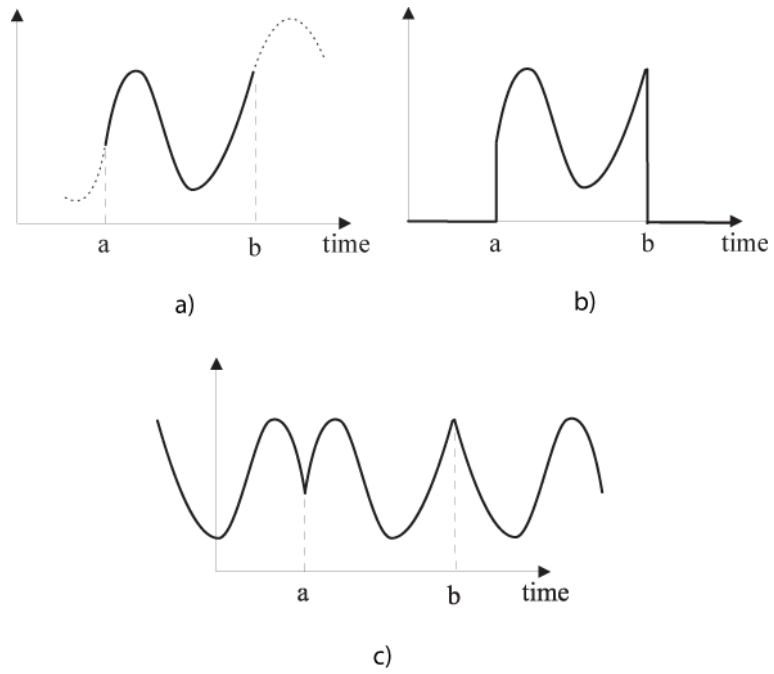

Fig. 1. Signal windowing: (a) Original signal, (b) Windowed signal, (c) $\widetilde{s}(t)$ for $t \in \mathbb{R}$

Note that possible discontinuities within the signal itself will not be solved in this way.

Since the Fourier transform is used for analytical continuation calculation, we try to have the support of the Fourier transform as compact and small as possible. The ideal case for calculation would be a Dirac in the Fourier domain. For complex time values, the spectrum is multiplied with a very fast increasing exponential, equation (29). Reduction of the spectrum support involves the reduction of the range of this exponential and the amplification of the noise. The noise sensibility problem is described in section IV-B.

Example with $\widetilde{GCM_4^2}$

By using moment (22), a distribution concentrated along the instantaneous frequency rate will be obtained. To compute it, one should calculate $s(t+jm)$ over the needed complex plane points. In order to simplify the calculation, in this case, we will present another solution. First, compute half part of the moment which is a function of real variables:

$$M(t,\tau) = s(t+\sqrt{\frac{\tau}{2}})s(t-\sqrt{\frac{\tau}{2}}). \qquad (31)$$

This part of the moment also provides a distribution more or less concentrated along half of the frequency rate (as much as Wigner-Ville distribution is concentrated along instantaneous frequency). It means that for a given time instant t, $\mathfrak{F}_\tau(M(t,\tau))$ is more concentrated than the Fourier transform of $s(t)$. Therefore, it is numerically easier to compute its analytical continuation $M(t,-\tau)$ than the analytical continuation of signal $s(t+j\tau)$. We will then compute $\widetilde{GCM_4^2}$ as:

$$\widetilde{GCM_4^2}[s](t,\tau) = M(t,\tau)M(t,-\tau)^*. \qquad (32)$$

Similar optimizations can be defined for the other complex time distributions. For example, in the case of time-frequency distributions, we have:

$$GCM_{2N}^1(t,\tau) = GCM_N^1\left(t,\frac{\tau}{2}\right) \times GCM_N^1\left(t,\frac{\tau}{2}\omega_{2N,1}\right)^{\omega_{2N,1}^*}. \qquad (33)$$

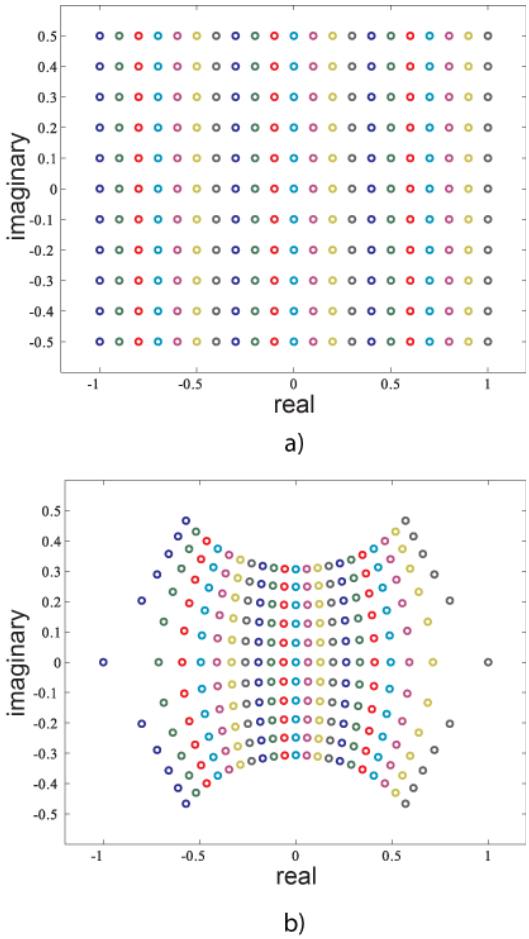

Fig. 2. Correspondance of complex-time planes

B. *Noise and sampling frequency influence on analytical continuation*

If the noise is present, it will be highly amplified for high frequencies due to multiplication by exponential function in (29). Thus, a slight noise in the high frequency range of the spectrum will have stronger influence than a strong signal at the lower frequencies. An illustration is presented in Fig. 3. In this case ($m = 0.12$), the exponential takes high values for negative part of the spectrum. At the beginning of the negative frequency part, the signal is correctly multiplied with the exponential. Then, as the signal has a fast decreasing spectrum, the multiplied spectrum tends toward zero. However, we observe a increased values at the end of the spectrum. It is due to the presence of noise. In this particular case, it would be easy to separate both parts of the spectrum, but when the noise level is higher, it is not so obvious. An efficient filtering becomes absolutely necessary.

Two interesting approaches are developed for efficient implementation of the complex-time distributions of noisy signals [6], [7]. In the first one, a region of support for complex-time distribution computation is obtained by using the short-time Fourier transform. Thus, the complex time distribution is computed, only, within the region where the short-time Fourier transform is above a certain threshold value, keeping complex argument small. The second method is based on the concept of cross complex-time distribution (similar with the cross Wigner-Ville based instantaneous frequency estimation [8]). An initial estimation is done by using any existing method and then the cross complex-time distribution is computed by using iterative procedure. In both approaches a high robustness to noise is achieved. These approaches, with corresponding quantitative analysis, can be used in the realization of the generalized complex-time distributions.

The sampling frequency also has an influence on the calculation. Indeed, when the spectrum is multiplied with $e^{-2\pi mk}$, some parts of the spectrum are revealed depending on the value of m. This effect is shown in Fig. 4. The top figure shows the multiplied spectrum for $m = 0$ which is the original spectrum. As m is increasing, the maximum shifts to the left on the frequency axis. As long as the multiplied spectrum vanishes before the end of the frequency axis, it is not a problem. However, one can see in the bottom figure, for $m = 0.3$, that one part of the multiplied spectrum is missing. In this case, the analytical continuation will be miscalculated.

As a consequence, the maximum value of m is mainly limited by the noise level but also by the sampling frequency.

In practical implementations, windowed forms of the time-frequency distributions are used. For the short time Fourier transform, the size of the window is subject to the trade

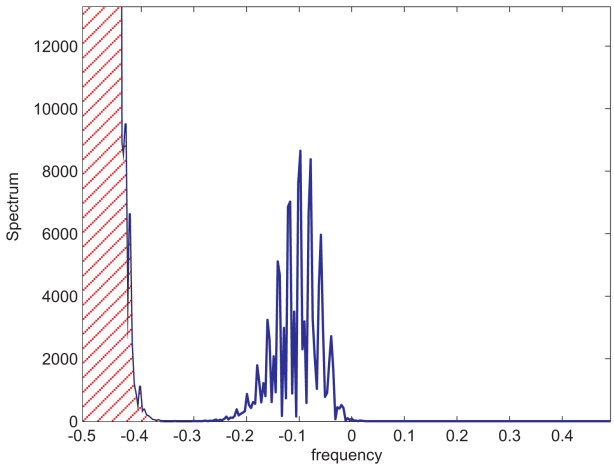

Fig. 3. Illustration of spectrum divergence due to noise

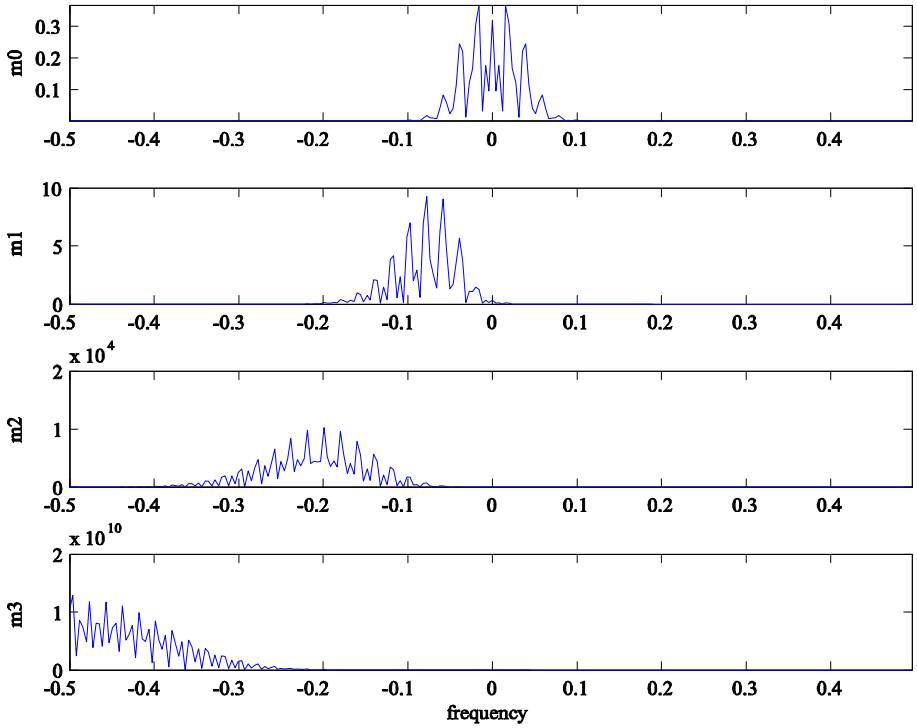

Fig. 4. Multiplied spectra : $S(k)e^{-2\pi mk}$

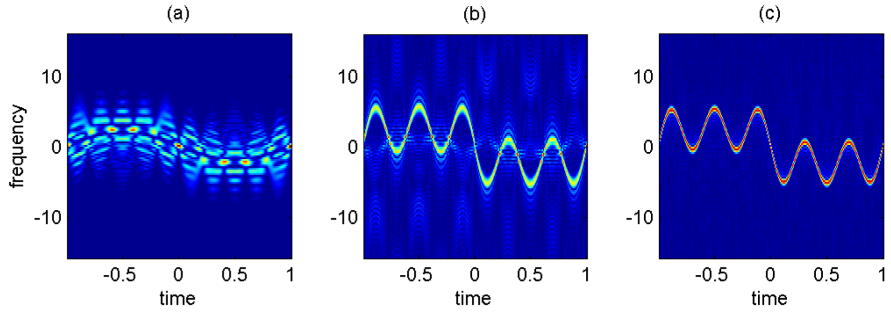

Fig. 5. Time-frequency representations: (a) WVD, (b) CTD, (c) 6^{th} GCD.

off between time and frequency resolutions. For the pseudo Wigner-Ville distribution, the choice is made assuming that the signal is a linear chirp within the windows. Since this hypothesis is weaker than stationarity, the length of the window can be increased in comparison to the spectrogram. It is possible to further reduce the negative influence of the window. Namely, the size of the window can be increased, by using the generalized complex moment, proportionally to the parameter N. In this way, the accuracy could be, theoretically, highly improved. However, numerical implementations introduce some limits for the size of the window in the GCM based distributions. It is especially important in order to avoid influence of the high values of m. In Section V, we will rather use equal size window for all distributions in order to compare interferences reduction.

V. Tests and illustrations

In this section we will test the presented complex-time distributions on several signals, including noisy ones. The results will be compared with conventional representations.

A. Signals

The distributions, introduced in this paper, are tested on the three signals described below:

$$\begin{aligned} s_1(t) &= e^{j(6cos(\pi t)+\frac{4}{3}cos(3\pi t)+\frac{4}{3}cos(5\pi t))} \\ s_2(t) &= s_1(t)+n(t) \\ s_3(t) &= e^{j(10cos(\pi t)+\frac{2}{3}cos(3\pi t)+cos(9\pi t))}. \end{aligned}$$

The first one is a periodically frequency modulated signal with rather rapid frequency variations. Noise is added in the second signal. The last one is still a periodically modulated signal with faster frequency variations. Note that, in real cases, these signals correspond to a radar signals produced by nonuniform rotation of a reflecting point. The normalized distance changes caused by the nonuniform rotation is described by $d(t) = 6cos(\pi t) + \frac{4}{3}cos(3\pi t) + \frac{4}{3}cos(5\pi t)$ in $s_1(t)$.

B. Instantaneous frequency representation

Various time-frequency representations of $s_1(t)$ are depicted in Fig. 5. The WVD cannot follow the frequency variation of the signal since it is highly non linear. The result is better with the CTD because the interferences are highly reduced. However they are still visible in the figure. Some of the artifacts, around zero frequency, are due to miscalculation of the analytical continuation. The sixth order GCD exhibits a better signal representation. It is almost interferences-free and has no artifacts in this case.

The signal $s_2(t)$ is contaminated with a white gaussian noise. The SNR is about 10dB. The WVD, the CTD and the sixth order GCD are shown in Fig. 6. The last representation is the best since the sixth order GCD is naturally more robust to noise than the CTD.

The last signal, $s_3(t)$, has very rapid frequency variations. It is used to show the limits of the CTD. The results are depicted in Fig. 7. The sixth order GCD is still well fitted to the theoretical instantaneous frequency and the interferences level is negligible compared with the WVD and the CTD.

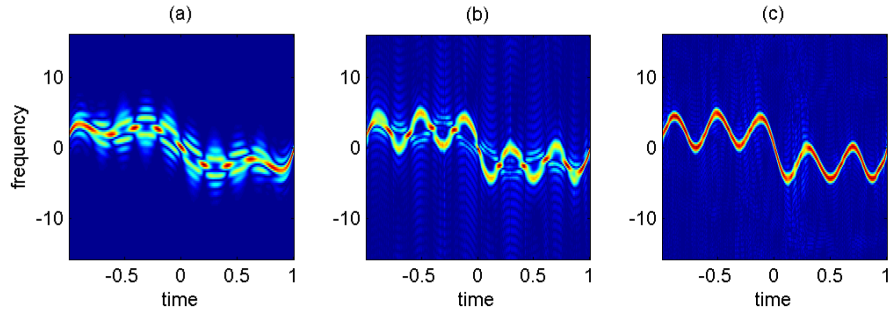

Fig. 6. Time-frequency representations of a noisy signal, SNR=10dB: (a) WVD, (b) CTD, (c) 6^{th} GCD.

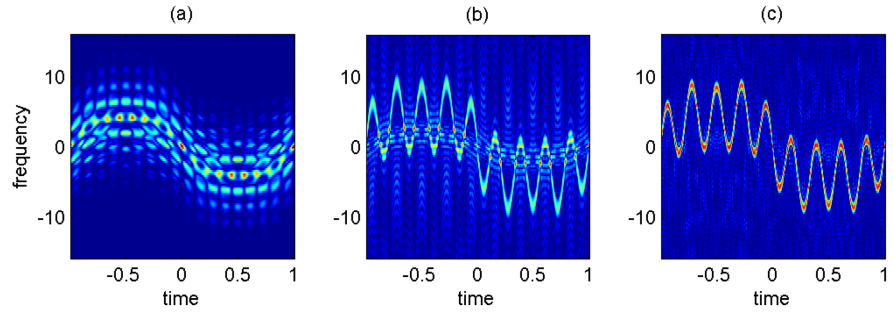

Fig. 7. Time-frequency representations of a signal with fast varying instantaneous frequency: (a) WVD, (b) CTD, (c) 6^{th} GCD.

C. Second and third phase derivatives

We now tackle the problem of higher order derivatives with second and third derivatives, $K = \{2, 3\}$. With $N = 2$, it is still possible to compute instantaneous frequency rate, since we must have $K \leq N$. To illustrate the concept, we applied $\widetilde{GCM}_2^2$, $\widetilde{GCM}_4^2$ and $\widetilde{GCM}_6^2$ on $s_1(t)$. The results are depicted in Fig. 8. A more significant smoothing has been used for this example. In Fig. 8.a, it is shown that the representation is more spread around instantaneous frequency rate, since the spread factor Q is more influential for this distribution. Fig. 8.b shows some artefact in the representation due to the analytical continuation approximations. In Fig. 8.c, we represent $\widetilde{GCD}_6^2$.

Note that the third phase derivative cannot be calculated with $N = 2$. We have to use at least $N = 3$, with $\widetilde{GCM}_3^3$. We will compare it to the $\widetilde{GCM}_4^3$ and $\widetilde{GCM}_6^6$. The distributions are applied on $s_1(t)$ as well. The first distribution, Fig. 10.a, shows better results than the second one, Fig. 10.b. Based on the order of the distribution, the opposite was expected. In fact, the analytical continuation of the second distribution is more difficult to compute due to the fourth unity roots location, implying some artifacts in the representation. The last figure, with sixth order representation, shows the best results.

Moreover, the position of the sixth unity roots in the complex plane is an asset compared with those of fourth order distribution, for example. Indeed, we will stay closer to the real axis when computing signal with complex argument, Fig. 9. As a consequence, the computation will be less sensitive to noise.

D. Example of instantaneous frequency rate estimation

Estimating the instantaneous frequency rate of a signal is also one of the topics. Some

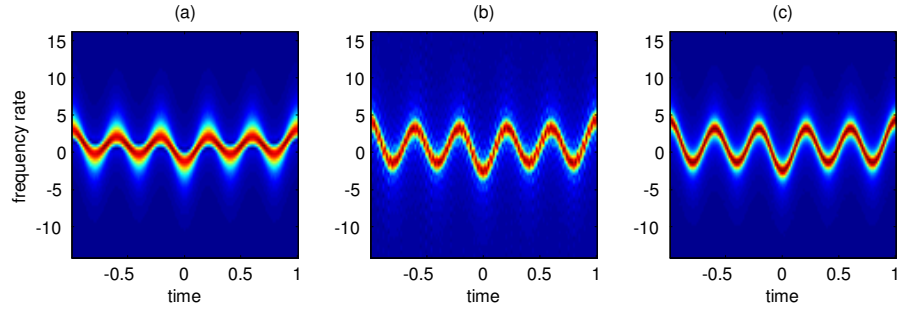

Fig. 8. Time-"frequency rate" representations: (a) 2^{nd} GCD, (b) 4^{th} GCD, (c) 6^{th} GCD.

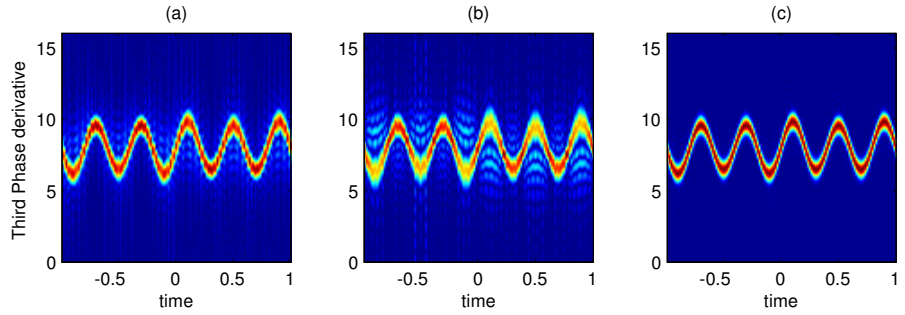

Fig. 10. Time-"third phase derivative" representations: (a) 3^{rd} GCD, (b) 4^{th} GCD, (c) 6^{th} GCD.

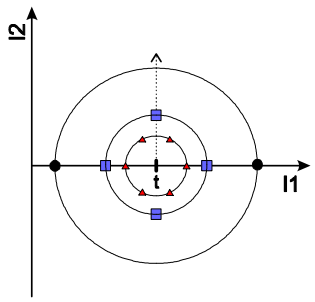

Fig. 9. Second order (•), fourth order (■) and sixth order (▲) unity roots divided by N

methods use directly the representation to extract the parameter. With the moments introduced in this paper, we can obtain representations concentrated along the instantaneous phase derivative. In other words, for any time value, the τ variable dependent signal $\widetilde{GCM}_N^K[s](t,\tau)$ is almost monochromatic. As a consequence, it is possible to use a parametric method like MUSIC algorithm to estimate its frequency. We applied MUSIC algorithm for the three moments dedicated to frequency rate estimation. These moments were applied to $s_1(t)$. The results are depicted in Fig. 11. A signal without noise is used to show the accuracy of estimation for a highly non linear phase. The estimation related to sixth order moment is almost identical to the theoretical law in the figure. For the second order moment, results are not so good. This was expected since, in Fig. 8.a, the representation is not correctly focused on the frequency rate.

VI. Conclusion

In this paper, a class of generalized complex lag distributions is proposed. These distributions are parameterized by two integers K and N. One important property is that they provide high concentration along the K^{th} derivative of the phase. A special case of this class of distributions, for $K = 1$, provides distributions for time-frequency analysis. Among them, the Wigner-Ville distribution is one of the special cases. The most interesting dis-

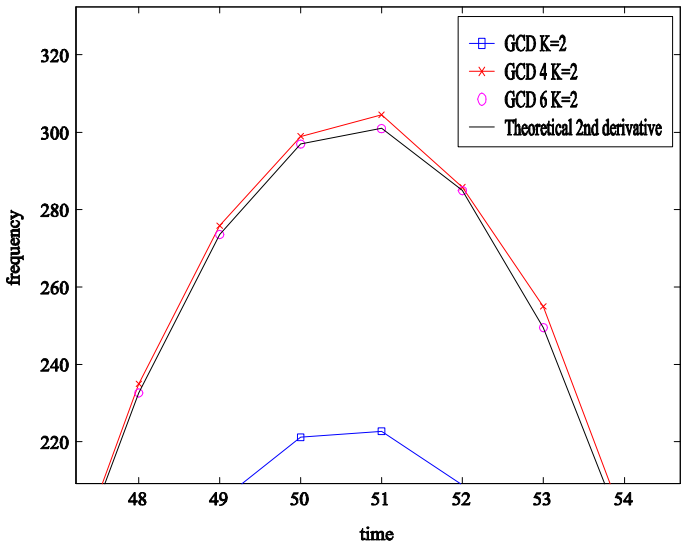

Fig. 11. Instantaneous frequency rate estimation.

tributions for $K = 2$ (time-"frequency rate" analysis) and for $K = 3$ are analyzed. The theory is illustrated and justified by numerical examples. Future work could be focused on detailed noise analysis and multicomponent signals.

Acknowledgment

This work was supported by the joint French-Montenegrin project "Pelikan".

References

[1] L. Cohen, *Time Ű Frequency Analysis*, Englewood Cliffs, NJ: Prentice- Hall, 1995.

[2] B. Boashash, *Time Ű Frequency Signal Analysis and Processing*, Amsterdam, The Netherlands: Elsevier, 2003.

[3] P. OŠShea, "A new technique for instantaneous frequency rate estimation," *in IEEE Signal Process. Lett.*, 2002, vol. 9, no. 8, pp. 251Ű252.

[4] S. Stankovic and L. Stankovic, "Introducing timeŰfrequency distribution with a complex-time argument," *IEE Electron. Lett.*, vol. 32, no. 14, pp. 1265Ű1267, Jul. 1996.

[5] W. Rudin, *Real and Complex Analysis*. New York: McGraw-Hill, 1987.

[6] L. Stankovic, "TimeŰfrequency distributions with complex argument," *IEEE Trans. Signal Process.*, vol. 50, no. 3, pp. 475Ű486, Mar. 2002.

[7] G. Viswanath and T. V. Sreenivas, "If estimation using higher order TFRS," *in Signal Process.*, Feb. 2002, vol. 82, no. 2, pp. 127Ű132.

[8] B. Boashash and P. OŠShea, "Use of cross WignerŰVille distribution for instantaneous frequency estimation," *IEEE Trans. Signal Process.*, vol. 41, no. 3, pp. 1439Ű1445, Mar. 1993.